

with a 2-mm entrance pupil illuminated by either a 900-W Xe arc lamp or by 75-W Xe and 100-W Hg arc lamps. Wavelengths were selected by the use of interference filters with full-width at half-maximum bandwidths of between 7 and 11 nm (Ealing or Oriol). The radiance of each beam could be controlled by the insertion of fixed neutral density filters (Oriol) or by the rotation of circular, variable neutral density filters (Rolyn Optics). Sinusoidal modulation was produced by the pulse-width modulation of fast, liquid crystal light shutters (Displaytech) at a carrier frequency of 400 Hz (which is much too fast to be resolved). The position of the observer's head was maintained by a dental wax impression. The experiments were under computer control. These systems are described in more detail elsewhere (Stockman, Plummer, & Montag, 2005).

Stimuli

The experimental conditions were chosen to favor measurements of the temporal properties of the long-wavelength-sensitive (L-) or middle-wavelength-sensitive (M-) cones. A flickering target of 4° of visual angle in diameter and either 650 or 589 nm in wavelength was presented in the center of a 9° diameter background field of 480 nm. Fixation was central. The 480-nm background, which delivered 8.26 log quanta s⁻¹ deg⁻² at the cornea, served primarily to suppress the rods (which function normally in these observers). In addition, the wavelength of the primary target (650 nm) was chosen to favor detection by cones rather than rods. The secondary target wavelength of 589 nm was used to determine the relative spectral sensitivity of the mechanism mediating flicker detection at 650 and 589 nm. As a further control to ensure that rods were not contributing to some measurements, data with the 650-nm target were replicated for the fatter following an intense full-field white bleach. Measurements were made during the cone plateau between 3 and 7 min following the bleach when cones have recovered but rods have not. The bleach was a white Ganzfeld (full-field) bleach of 5.42 log scotopic trolands viewed for 30 s, which bleaches approximately 60% of the rod photopigment (Pugh, 1975a). This bleach suffices to elevate rod threshold substantially during the cone plateau and for many minutes thereafter (e.g., Pugh, 1975b).

For the critical flicker fusion measurements, target radiances were varied. For the modulation sensitivity measurements, a 650-nm target was used, fixed at a time-averaged radiance of 10.38 log quanta s⁻¹ deg⁻².

In a separate experiment to look for a short-wavelength-sensitive (S-) cone response in the affected observers, a flickering 4° target of 440 nm and variable radiance was presented in the center of a 9° background of 620 nm and 11.51 log₁₀ quanta s⁻¹ deg⁻². These conditions isolate the S-cone response in normals up to a 440-nm target radiance of about 10.5 log₁₀ quanta s⁻¹ deg⁻² (e.g., Stockman,

MacLeod, & DePriest, 1991; Stockman, MacLeod, & Lebrun, 1993; Stockman & Plummer, 1998). CFF measurements were made in both subjects over a range of 440 nm radiances, but no S-cone response could be measured.

The auditory stimulus for the visual–auditory phase matching experiment was produced by sending 2.5 ms square-wave pulses to a buzzer at the desired pulse rate. Thus, the “clicker” was a pulsed, broadband auditory stimulus. The visual stimuli for this experiment were the same as for the modulation sensitivity measurements, except that the modulation, in order to be visible, was set slightly suprathreshold.

Procedures

Before making any measurements, subjects light adapted to the stimuli for at least 3 min. They interacted with the computer by means of buttons and received feedback and instructions by means of tones and a computer-controlled voice synthesizer. Three types of measurements were made: (i) critical flicker fusion, in which the observers adjusted the flicker frequency (at the fixed maximum stimulus modulation of 92%) to find the frequency at which the flicker just disappeared; (ii) modulation threshold, in which the observers adjusted the flicker modulation (at a fixed frequency) to find the modulation at which the flicker just disappeared; and (iii) visual–auditory phase matching, in which auditory clicks were adjusted in phase to align perceptually with a distinct phase of the perceived flicker cycle (Stockman, Williams, & Smithson, 2004). In the last of these, the alignment setting was recorded relative to the *peak* of the perceived flicker. In practice, the subject aligned the click to the flicker iteratively using *both* the peak and the trough of the visible flicker cycle. That is, he first aligned the click with the peak, then shifted the phase of the visible flicker by 180° by pressing a button and now aligned the click with the trough, then again shifted the phase of the flicker by 180° and aligned the click with the peak, and so on. Using both phases to align the click proved more reliable than using just one. Settings could be made reliably in these experiments at frequencies up to 1 Hz.

Each data point is the average of three or four independent measurements, each of which is the average of three settings. The error bars are ±1 standard error of measurement (*SEM*).

Calibration

The radiant fluxes of test and background fields were measured at the plane of the observer's entrance pupil with a UDT Radiometer that had been calibrated by the manufacturer against a standard traceable to the National Bureau of Standards and cross-calibrated by us against our own radiometric standard (Gamma Scientific, San Diego).

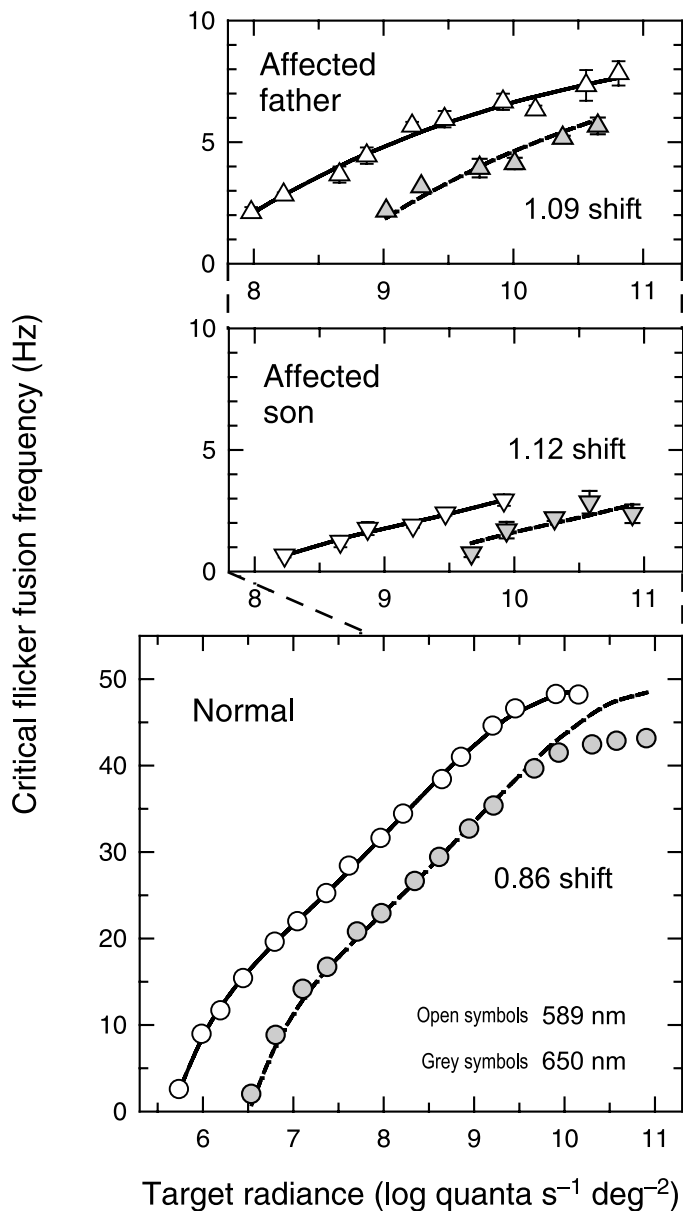


Figure 3. Cone CFF data for a normal observer (circles) and for the affected father (triangles) and son (inverted triangles). Measurements were made on a 481-nm background of 8.26 log quanta $s^{-1} \text{ deg}^{-2}$. The grey symbols are the 650-nm target data replotted from Figure 1. The open symbols are comparable data obtained with a 589-nm target. The functions denoted by the continuous lines are arbitrary functions chosen to describe the 589-nm CFF data for each subject. The functions denoted by the dashed lines are the 589-nm functions for each subject shifted along the log radiance axis to best fit their 650-nm data. The shifts listed in the figure reflect the spectral sensitivity difference between 589 and 650 nm for the CFF measurements.

for the normal and 1.09 and 1.12, respectively, for the affected father and son. In terms of photoreceptor spectral sensitivities, the shifts are consistent with a mixed L- and M-cone detection of flicker in all subjects, with detection in the normal being more L-cone dominated than in the

affected father and son. Thanks to the large discrepancies between the measured spectral sensitivity differences and the rod and S-cone predictions, we can rule out any significant involvement of those photoreceptors in the detection of 650-nm flicker. Moreover, the similarity in shape of the curve fitted to the 589-nm CFF data to that fitted to the 650-nm data, both for the father and son, is also consistent with the detection of 589 nm flicker being cone mediated. We can also exclude more exotic possibilities, such as ganglion cells containing melanopsin, because the λ_{max} of melanopsin of approximately 480 nm (see Berson, 2003) is intermediate between the rods and S-cones and would produce a much greater shift than we find.

In a series of S-cone CFF measurements over a wide range of S-cone adaptation levels, no evidence for any S-cone response could be found. It is possible that a response might be found at high S-cone bleaching levels, but such levels are considered to be potentially damaging and were not used in our experiments.

Cone modulation sensitivity functions

The CFF functions provide information about sensitivity at the temporal resolution limit, but not at lower temporal frequencies. To investigate the properties of the mechanisms mediating detection at lower temporal frequencies, we measured cone modulation sensitivities. A fixed time-averaged 650-nm radiance of 10.38 log quanta $s^{-1} \text{ deg}^{-2}$ was chosen. Like the CFF functions, the modulation sensitivities were measured on the 480-nm background.

Figure 4 shows temporal modulation sensitivities for the affected father (gray triangles), the affected son (inverted filled triangles), and the normal (open circles). The lower panel shows the data for all three observers, while the upper panel replots the data for the affected individuals at a larger scale. The data for the normal are typical for this adaptation level, peaking at approximately 7 Hz and extending to approximately 45 Hz (e.g., De Lange, 1958; Kelly, 1961). Functions like these that peak at intermediate frequencies are known as bandpass. The data for the affected individuals, as expected from the CFF measurements, are atypical. Their data extend to only 6 Hz for the father and 2 Hz for the son. In contrast to the normal bandpass sensitivity function, their sensitivity follows a “low pass” function that falls monotonically with temporal frequency. The differences between the father and son can be accounted for mainly by an overall loss of sensitivity. This is illustrated in the lower panel, in which the father’s data have been vertically shifted to align with the son’s data as shown by the dashed line. The best-fitting vertical shift is 0.58 log unit (i.e., a shift equivalent to an attenuation factor of 3.8).

At the lowest frequency of 0.25 Hz, the sensitivities for the affected father and son are about 3 and 10 times

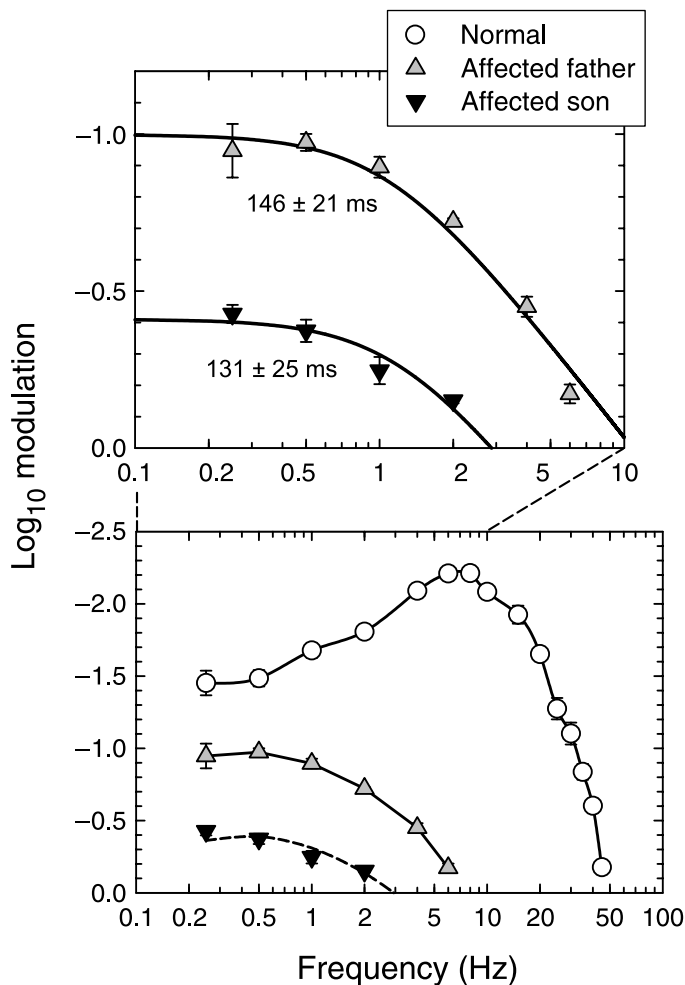


Figure 4. Cone modulation sensitivity data for a normal (circles) and for the affected father (triangles) and son (inverted triangles) measured using a modulated 650-nm target with a time-averaged radiance of $10.38 \log \text{ quanta s}^{-1} \text{ deg}^{-2}$ superimposed on a 481-nm background of $8.26 \log \text{ quanta s}^{-1} \text{ deg}^{-2}$. The data for the affected observers are plotted in both panels at different scales. In the lower panel, the data for the normal and the father are connected by continuous lines. The father's data, as shown by the dashed line, have been vertically shifted by 0.58 log unit to align with the data for the son. In the upper panel, best-fitting versions of a model describing the behavior of a single leaky integrator (see Equation 1) are shown as the continuous lines. The best-fitting time constants ($\pm 1 \text{ SE}$) are noted in the panel.

lower, respectively, than that of the normal. This suggests that the father and son are able to see steady lights (0 Hz) of high radiance reasonably well. Motion or flicker that depends on temporal frequency components much above 1 or 2 Hz, however, will be largely invisible to them.

If we suppose that the temporal modulation sensitivity functions for the affected father and son depend upon light-induced changes in the amount of a particular photoproduct that activates the transduction cascade

(which we shall refer to as X^* for short), then the shapes of those functions should reflect the rate of production and decay of X^* (in fact, they should be related to the Fourier transform of the lifetime of X^*). The lifetime of X^* should in turn depend on the convolution of the reaction time constants up to and including the removal of X^* itself (e.g., Baylor, Hodgkin, & Lamb, 1974; Fourtes & Hodgkin, 1964). Since we are making *psychophysical* measurements, the modulation sensitivities may also reflect the temporal properties of processes in the cascade subsequent to the secondary activation by X^* as well as those at postreceptor neural stages. Potentially, then, the modulation sensitivities measured in the father and son could be complex; but, intriguingly, they are not.

We find that the modulation sensitivity data can be accounted for by a model in which the amount of the activating photoproduct, X^* , is limited by a simple first-order reaction, the effect of which is comparable to that of a single leaky integrator (RC filter) with exponential decay, and with a single time constant. To evaluate this model, we fitted the standard formula for a leaky integrator (e.g., Watson, 1986) separately to the data for the father and son. The formula for the amplitude response, $A(f)$, of a single leaky integrator is

$$A(f) = \tau[(2\pi f\tau)^2 + 1]^{-0.5}, \quad (1)$$

where f is the frequency in Hertz and τ is the time constant in seconds. The fits were carried out to the logarithmic modulation thresholds as shown in Figure 3. In addition to varying τ , an additional sensitivity scaling factor (vertical logarithmic shift) was allowed. The results of the model fits, which are shown by the solid lines in the upper panel, are remarkably good with root-mean-squared errors of only 0.044 (father) and 0.031 (son) and R^2 values of 0.977 (father) and 0.915 (son). The estimated time constants (plus and minus the standard error of the fit) are $146 \pm 21 \text{ ms}$ (father) and $131 \pm 25 \text{ ms}$ (son), a similarity that suggests the kinetics of the limiting reaction are essentially the same for both observers. Different vertical shifts of -1.84 ± 0.04 for the father and -1.29 ± 0.06 for the son reflect their different sensitivities. Comparable data from normals are bandpass and are far too complex to be modelled by a single leaky integrator stage (e.g., De Lange, 1958).

The fact that the data can be accounted for by a simple first order reaction, although the amount of X^* should depend on the convolution of the preceding reaction time constants, and on the time constants of later processes, suggests two things: first, that the time constant of the limiting reaction of 140 ms is much longer than those of any other relevant process; and second, that the time constants of the other stages are too short to produce any sizeable *frequency-dependent* effects on modulation sensitivity in the visible range of frequencies, which in this

case are those up to and including 6 Hz (see Figure 3). (For reference, a time constant of 20 ms would reduce the sensitivity at 6 Hz by 0.1 log unit, relative to sensitivity at 0 Hz.)

In a linear system, the order of the reactions can be changed without affecting the result (see Baylor et al., 1974, p. 702), so that we do not know where the dominant (slowest) limiting stage in the reaction cascade is with respect to X^* . On the assumption that it would be inefficient to follow a slow process with a faster one, and extrapolating from the known tendency for successive steps in the retinoid cycle to become slower (Lamb & Pugh, 2004), we speculate that the most plausible limiting stage is the decay of X^* itself.

Visual–auditory phase matching

Modulation sensitivity data, such as those shown in Figure 4, provide only a partial picture of the visual response. A more complete picture requires knowledge also of the visual delay. If vision is limited by a first order reaction with a time constant of approximately 140 ms, then the effects of that reaction should also be evident in the delay of the visual response. Specifically, the response of the affected subjects should be phase delayed [$P(f)$] with respect to the normal by

$$P(f) = \tan^{-1}(2\pi f\tau), \quad (2)$$

where f is the frequency in Hertz and τ is the time constant in seconds ($\tau = 0.146$ s, for the affected father).

In psychophysics, phase delays must be measured relative to a second perceptual process. Moreover, to enable comparisons between the affected subjects and normals, that second process must be common to both groups. We therefore measured visual delays relative to an auditory reference stimulus produced by a train of clicks (clicker). Rate matching between flicker and clicker has been reported before (e.g., Bowker & Mandler, 1981; Fukuda, 1977; Gebhard & Mowbray, 1959; Shipley, 1964), but phase matching seems uncommon. In a preliminary study, we reported that phase matching in normal observers is roughly veridical at temporal frequencies below approximately 1.5 Hz but breaks down at higher frequencies, where only rate matching is possible (Stockman et al., 2004). Although limited to 1 Hz and below, the visual–auditory phase matching data reported here provide a strong test of the hypothesis that the visual response in the affected father is rate-limited by a sluggish reaction.

Figure 5 shows the visual–auditory phase delays for the normal (open circles) and the affected father (gray triangles). The visual stimuli were the same as those for the modulation sensitivity measurements shown in Figure 4, except that the flicker modulation was set to

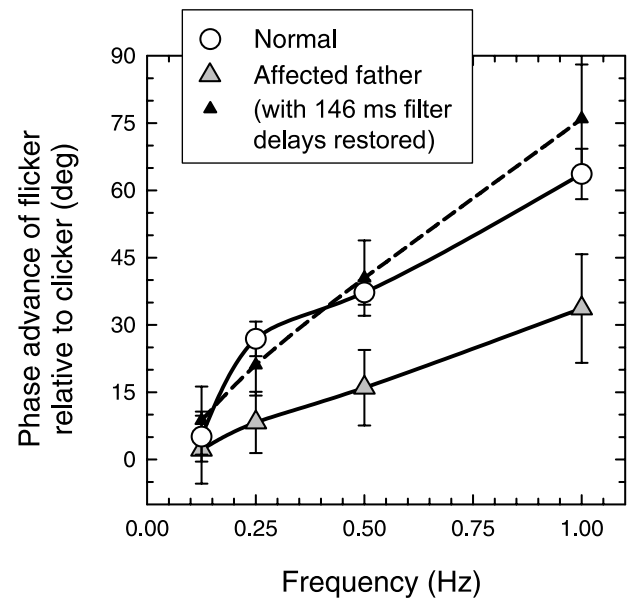


Figure 5. Phase advance of flicker needed to align peak with an auditory click for the affected father (gray diamonds) and the normal (open circles). The filled triangles show the data for the father phase advanced to compensate for the phase delays assumed to be caused by the limiting reaction. Visual stimuli as for Figure 4.

be slightly suprathreshold in order to be visible. The phase data for the normal are clearly more advanced than those for the father by up to approximately 30° by 1 Hz. When the father's data are advanced (filled triangles, dashed line) to compensate for the phase delays introduced by a leaky integrator with a time constant of 146 ms (Equation 2), the affected and normal phase data align well. We conclude therefore that both the modulation sensitivity and the phase delay data are consistent with vision in the affected observer being limited by a sluggish first order reaction.

The phase measurements also provide an important control for an alternative explanation of the modulation sensitivity functions for the affected observers: that their shapes depend on an early internal noise source rather than being limited by a first order reaction. As pointed out theoretically (Graham & Hood, 1992) and shown experimentally (Rovamo, Raninen, & Donner, 1999; Rovamo, Raninen, Lukkarinen, & Donner, 1996), flicker modulation sensitivity functions measured in the presence of dominant early noise may not carry information about the shape of the underlying temporal filter. Since dominant early noise in the transduction cascade might be an indirect consequence of the Ga mutation, we were concerned that such noise may be affecting our results. However, given that any early noise should affect modulation sensitivities, but not phase delays, this alternative explanation is not supported by our combined

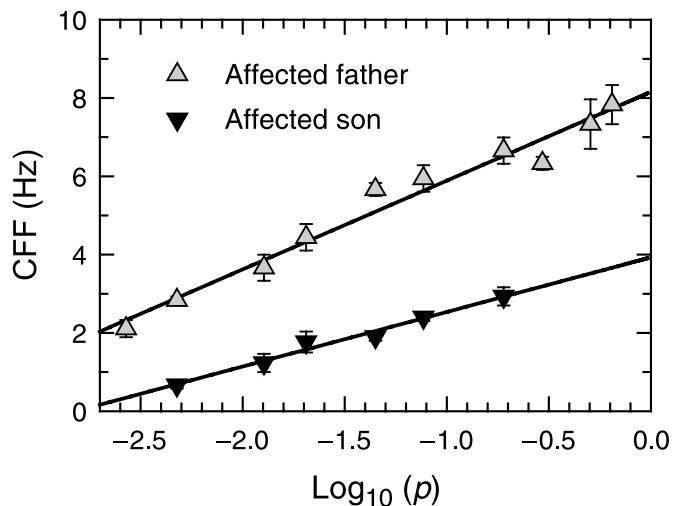


Figure 6. CFF data for the affected father (triangles) and son (inverted triangles) measured with the 589-nm target plotted as a function of the logarithm of the fraction of bleached pigment. Data replotted from Figure 2. The fraction of bleached pigment was calculated using standard bleaching equations and assuming a 50% bleach at 4.3 log trolands (Rushton & Henry, 1968). The continuous lines are best-fitting versions of Equation 3.

We note that there is not necessarily any inconsistency between Equation 3, which relates sensitivity to $\log(p)$, and the Dowling–Rushton equation, which relates sensitivity loss to 10^p (Dowling, 1960; Rushton, 1961). The former is assumed to depend on an early photoproduct with a time constant of decay of 140 ms, whereas the latter will also reflect the prolonged desensitization caused by more sluggishly removed photoproducts, such as the opsin.

The affected father is about 4 times more sensitive to cone stimuli than his son. We are not certain of the origin of this difference, or even whether it is receptor or postreceptor. Importantly, though, the inferred time constants from the modulation sensitivity measurements for the two observers are the same. Thus, although their overall sensitivities differ, the biochemical processes underlying their vision do not.

Identification of the limiting reaction

Our data suggest that the amount of X^* is limited by a reaction with a time constant of approximately 140 ms that is substantially slower than other reaction steps. Given that successive steps in the retinoid cycle tend to become progressively slower (e.g., Lamb & Pugh, 2004), the time constant of 140 ms is likely to pertain to the decay of X^* .

In principle, all we need do to identify X^* is to find the relevant reaction in the cone retinoid cycle with a time constant close to 140 ms. In practice, however, such an

identification is far from straightforward. First, most relevant data are from rods, which dark adapt more slowly than cones. Second, most photochemical data were obtained at low temperatures under physiologically unrealistic conditions, such as in detergent solution. Consequently, estimates of the time constants of decay will substantially underestimate those likely to be found in photoreceptors at body temperature. And, indeed, the available estimates of the time constants of decay of meta-II and meta-III are too slow to account for our data (see Table 1 of Imai et al., 2005).

Nonetheless, new data obtained using a fast CCD spectrophotometer with chicken green cone pigment expressed in HEK293 cells reveal a time constant of decay of meta-II of 960 ± 460 ms at 2 °C (Kuwayama, Imai, Morizumi, & Shichida, 2005). It seems plausible therefore that human cone pigment meta-II might decay with a time constant of 140 ms at 37°C, since this would require less than a doubling of the reaction rate for every 10 °C rise. Therefore, we tentatively identify X^* as the decay of cone meta-II by the hydrolysis of the Schiff-base bond that attaches the chromophore. However, recent microspectrophotometric measurements of meta-I and meta-II decay in single goldfish cones carried out at 20 °C can be fitted by two exponentials, of which the faster has a time constant of 5.1 s (Golobokova & Govardovski, 2006). Corrected to 37 °C, this is still slower than the rate we require to model our data.

There is relatively little psychophysical data on the dynamics of human cone dark adaptation. Perhaps the most relevant data are those of Pianta and Kalloniatis (2000), in which they identified two exponentially decaying components in the cone recovery curve: a faster component with a time constant of approximately 19 s, and a slower one with a time constant of approximately 51 s. Both of these are, however, too long to be consistent with the time constant of 140 ms inferred from the modulation sensitivity data (which is too short to have been revealed in their measurements). Pianta and Kalloniatis (2000) related their slower component to the decay of cone meta-II. Although time constants comparable to 19 s for some cone meta-II opsins are obtained using low temperature spectroscopy under nonphysiological conditions (see Table 1 of Imai et al., 2005), we believe that the decay of meta-II *in vivo* is likely to be faster.

Alternative Explanations

Although the vestigial cone-driven response is consistent with the secondary activation of the phototransduction cascade by a cone metarhodopsin photoproduct, other alternative explanations cannot be excluded. One possibility is that there is more than one cone GNAT2 gene in humans (Lerea, Bunt-Milam, & Hurley, 1989); at least one of which is spared in our subjects. Although some Southern blot analyses initially suggested that there could

- transduction in salamander cones. *Journal of General Physiology*, 106, 543–557. [[PubMed](#)] [[Article](#)]
- Crawford, B. H. (1937). The change of visual sensitivity with time. *Proceedings of the Royal Society of London, Series B: Biological Sciences*, B123, 69–89.
- Crawford, B. H. (1947). Visual adaptation in relation to brief conditioning stimuli. *Proceedings of the Royal Society of London, Series B: Biological Sciences*, B134, 283–302.
- De Lange, H. (1958). Research into the dynamic nature of the human fovea-cortex systems with intermittent and modulated light: I. Attenuation characteristics with white and colored light. *Journal of the Optical Society of America*, 48, 777–784. [[PubMed](#)]
- Dean, D. M., Nguiragool, W., Miri, A., McCabe, S. L., & Zimmerman, A. L. (2002). All-trans-retinal shuts down rod cyclic nucleotide-gated ion channel: A novel role for photoreceptor retinoids in the response to bright light? *Proceedings of the National Academy of Sciences of the United States of America*, 99, 8372–8377. [[PubMed](#)] [[Article](#)]
- Donner, K. O., & Reuter, T. (1967). Dark-adaptation processes in the rhodopsin rod's of the frog's retina. *Vision Research*, 7, 17–41. [[PubMed](#)]
- Dowling, J. E. (1960). Chemistry of visual adaptation in the rat. *Nature*, 188, 114–118. [[PubMed](#)]
- Fain, G. L., Matthews, H. R., Cornwall, M. C., & Koutalos, Y. (2001). Adaptation in vertebrate photoreceptors. *Physiological Reviews*, 81, 117–151. [[PubMed](#)] [[Article](#)]
- Ferry, J. (1892). Persistence of vision. *American Journal of Science and Arts*, 44, 192–207.
- Fourtes, M. G., & Hodgkin, A. L. (1964). Changes in time scale and sensitivity in the ommatidia of limulus. *Journal of Physiology*, 172, 239–263. [[PubMed](#)] [[Article](#)]
- Fukuda, T. (1977). Subjective frequency in flicker perception. *Perceptual and Motor Skills*, 45, 203–210. [[PubMed](#)]
- Gebhard, J. W., & Mowbray, G. H. (1959). On discriminating the rate of visual flicker and auditory flutter. *American Journal of Psychology*, 72, 521–529. [[PubMed](#)]
- Geisler, W. S. (1979). Evidence for the equivalent-background hypothesis in cones. *Vision Research*, 19, 799–805. [[PubMed](#)]
- Golobokova, E. Y., & Govardovskii, V. I. (2006). Late stages of visual pigment photolysis in situ: Cones vs. rods. *Vision Research*, 46, 2287–2297. [[PubMed](#)]
- Graboswki, S. R., & Pak, W. L. (1975). Intracellular recordings of rod responses during dark-adaptation. *Journal of Physiology*, 247, 363–391. [[PubMed](#)] [[Article](#)]
- Graham, N., & Hood, D. C. (1992). Quantal noise and decision rule in dynamic models of light adaptation. *Vision Research*, 32, 779–787. [[PubMed](#)]
- Hamer, R. D., Nicholas, S. C., Tranchina, D., Lamb, T. D., & Jarvinen, J. L. (2005). Toward a unified model of vertebrate rod phototransduction. *Visual Neuroscience*, 22, 417–436. [[PubMed](#)] [[Article](#)]
- He, Q., Alexeev, D., Estevez, M. E., McCabe, S. L., Calvert, P. D., Ong, D. E., et al. (2006). Cyclic nucleotide-gated ion channels in rod photoreceptors are protected from retinoid inhibition. *Journal of General Physiology*, 128, 473–485. [[PubMed](#)] [[Article](#)]
- Hecht, S., & Schlaer, S. (1936). Intermittent stimulation by light: V. The relation between intensity and critical frequency for different parts of the spectrum. *Journal of General Physiology*, 19, 965–977.
- Hecht, S., & Verrijp, C. D. (1933). The influence of intensity, color and retinal location on the fusion frequency of intermittent illumination. *Proceedings of the National Academy of Sciences of the United States of America*, 19, 522–535. [[PubMed](#)] [[Article](#)]
- Imai, H., Kuwayama, S., Onishi, A., Morizumi, T., Chisaka, O., & Shichida, Y. (2005). Molecular properties of rod and cone visual pigments from purified chicken cone pigments to mouse rhodopsin in situ. *Photochemical & Photobiological Sciences*, 4, 667–674. [[PubMed](#)]
- Kelly, D. H. (1961). Visual responses to time-dependent stimuli: I. Amplitude sensitivity measurements. *Journal of the Optical Society of America*, 51, 422–429. [[PubMed](#)]
- Kuwayama, S., Imai, H., Morizumi, T., & Shichida, Y. (2005). Amino acid residues responsible for the meta-III decay rates in rod and cone visual pigments. *Biochemistry*, 44, 2208–2215. [[PubMed](#)]
- Lamb, T. D., & Pugh, E. N., Jr. (2004). Dark adaptation and the retinoid cycle of vision. *Progress in Retinal and Eye Research*, 23, 307–380. [[PubMed](#)]
- Leibrock, C. S., & Lamb, T. D. (1997). Effect of hydroxylamine on photon-like events during dark adaptation in toad rod photoreceptors. *Journal of Physiology*, 501, 97–109. [[PubMed](#)] [[Article](#)]
- Leibrock, C. S., Reuter, T., & Lamb, T. D. (1994). Dark adaptation of toad rod photoreceptors following small bleaches. *Vision Research*, 34, 2787–2800. [[PubMed](#)]

- Leibrock, C. S., Reuter, T., & Lamb, T. D. (1998). Molecular basis of dark adaptation in rod photoreceptors. *Eye*, *12*, 511–520. [[PubMed](#)]
- Lerea, C. L., Bunt-Milam, A. H., & Hurley, J. B. (1989). Alpha-transducin is present in blue-, green-, and red-sensitive cone photoreceptors in the human retina. *Neuron*, *3*, 367–376. [[PubMed](#)]
- Liu, Y., Arshavsky, V. Y., & Ruoho, A. E. (1996). Interaction sites of the COOH-terminal region of the gamma subunit of cGMP phosphodiesterase with the GTP-bound alpha subunit of transducin. *Journal of Biological Chemistry*, *271*, 26900–26907. [[PubMed](#)] [[Article](#)]
- Matthews, H. R., Cornwall, M. C., & Fain, G. L. (1996). Persistent activation of transducin by bleached rhodopsin in salamander rods. *Journal of General Physiology*, *108*, 557–563. [[PubMed](#)] [[Article](#)]
- McCabe, S. L., Pelosi, D. M., Tetreault, M., Miri, A., Nguitragool, W., Kovithathanaphong, P., et al. (2004). All-trans-retinal is a closed-state inhibitor of rod cyclic nucleotide-gated ion channels. *Journal of General Physiology*, *123*, 521–531. [[PubMed](#)] [[Article](#)]
- Melia, T. J., Jr., Cowan, C. W., Angleson, J. K., & Wensel, T. G. (1997). A comparison of the efficiency of G protein activation by ligand-free and light-activated forms of rhodopsin. *Biophysical Journal*, *73*, 3182–3191. [[PubMed](#)] [[Article](#)]
- Michaelides, M., Aligianis, I. A., Holder, G. E., Simunovic, M., Mollon, J. D., Maher, E. R., et al. (2003). Cone dystrophy phenotype associated with a frameshift mutation (M280fsX291) in the alpha-subunit of cone specific transducin (GNAT2). *British Journal of Ophthalmology*, *87*, 1317–1320. [[PubMed](#)] [[Article](#)]
- Morris, T. A., & Fong, S. L. (1993). Characterization of the gene encoding human cone transducin alpha-subunit (GNAT2). *Genomics*, *4*, 442–448. [[PubMed](#)]
- Pepperberg, D. R., Lurie, M., Brown, P. K., & Dowling, J. E. (1976). Visual adaptation effects of externally applied retinal on the light-adapted isolated skate retina. *Science*, *191*, 394–396. [[PubMed](#)]
- Pianta, M. J., & Kalloniatis, M. (2000). Characterisation of dark adaptation in human cone pathways: An application of the equivalent background hypothesis. *Journal of Physiology*, *528*, 591–608. [[PubMed](#)] [[Article](#)]
- Porter, T. C. (1902). Contributions to the study of flicker: II. *Proceedings of the Royal Society of London*, *A70*, 313–319.
- Pugh, E. N. (1975a). Rhodopsin flash photolysis in man. *Journal of Physiology*, *248*, 393–412. [[PubMed](#)] [[Article](#)]
- Pugh, E. N. (1975b). Rushton's Paradox: Rod dark adaptation after flash photolysis. *Journal of Physiology*, *248*, 413–431. [[PubMed](#)] [[Article](#)]
- Pugh, E. N., Jr., & Lamb, T. D. (2000). Phototransduction in vertebrate rods and cones: Molecular mechanisms of amplification, recovery and light adaptation. In D. G. Stavenga, W. J. de Grip, & E. N. Pugh (Eds.), *Handbook of biological physics: Vol. 3. Molecular mechanisms of visual transduction* (pp. 183–255). Amsterdam: Elsevier.
- Pugh, E. N., Jr., Nikonov, S., & Lamb, T. D. (1999). Molecular mechanisms of vertebrate photoreceptor light adaptation. *Current Opinion in Neurobiology*, *9*, 410–418. [[PubMed](#)]
- Rovamo, J., Raninen, A., & Donner, K. (1999). The effects of temporal noise and retinal luminance on foveal flicker sensitivity. *Vision Research*, *39*, 533–539. [[PubMed](#)]
- Rovamo, J., Raninen, A., Lukkarinen, S., & Donner, K. (1996). Flicker sensitivity as a function of spectral density of external white temporal noise. *Vision Research*, *36*, 3767–3774. [[PubMed](#)]
- Rushton, W. A. (1961). Dark-adaptation and the regeneration of rhodopsin. *Journal of Physiology*, *156*, 166–178. [[PubMed](#)] [[Article](#)]
- Rushton, W. A., & Henry, G. H. (1968). Bleaching and regeneration of cone pigments in man. *Vision Research*, *8*, 617–631. [[PubMed](#)]
- Shipley, T. (1964). Auditory flutter-driving of visual flicker. *Science*, *145*, 1328–1330. [[PubMed](#)]
- Stiles, W. S., & Crawford, B. H. (1932). Equivalent adaptation levels in localised retinal areas. In *The Physical and Optical Societies Report* (pp. 194–211). Cambridge: Cambridge University Press.
- Stockman, A., MacLeod, D. I., & DePriest, D. D. (1991). The temporal properties of the human short-wave photoreceptors and their associated pathways. *Vision Research*, *31*, 189–208. [[PubMed](#)]
- Stockman, A., MacLeod, D. I., & Lebrun, S. (1993). Faster than the eye can see: Blue cones respond to rapid flicker. *Journal of the Optical Society of America A, Optics and Image Science*, *10*, 1396–1402. [[PubMed](#)]
- Stockman, A., & Plummer, D. J. (1998). Color from invisible flicker: A failure of the Talbot–Plateau law caused by an early ehardf saturating nonlinearity used to partition the human short-wave cone pathway. *Vision Research*, *38*, 3703–3728. [[PubMed](#)]
- Stockman, A., & Plummer, D. J. (2005a). Long-wave-length adaptation reveals slow, spectrally-opponent inputs to the human luminance pathway. *Journal of Vision*, *5*(9):5, 702–716, <http://journalofvision.org/5/9/5/>, doi:10.1167/5.9.5. [[PubMed](#)] [[Article](#)]

- Stockman, A., & Plummer, D. J. (2005b). Spectrally-opponent inputs to the human luminance pathway: Slow +L and –M cone inputs revealed by low to moderate long-wavelength adaptation. *Journal of Physiology*, 566, 77–91. [[PubMed](#)] [[Article](#)]
- Stockman, A., Plummer, D. J., & Montag, E. D. (2005). Spectrally-opponent inputs to the human luminance pathway: Slow +M and –L cone inputs revealed by intense long-wavelength adaptation. *Journal of Physiology*, 566, 61–76. [[PubMed](#)] [[Article](#)]
- Stockman, A., & Sharpe, L. T. (2000). The spectral sensitivities of the middle- and long-wavelength sensitive cones derived from measurements in observers of known genotype. *Vision Research*, 40, 1711–1737. [[PubMed](#)]
- Stockman, A., Williams, M. R., & Smithson, H. E. (2004). Flicker-clicker: Cross modality matching experiments [[Abstract](#)]. *Journal of Vision*, 4(11):86, 86a, <http://journalofvision.org/4/11/86/>, doi:10.1167/4.11.86.
- Watson, A. B. (1986). Temporal sensitivity. In K. Boff, L. Kaufman, & J. Thomas (Eds.), *Handbook of perception and human performance* (vol. 1, pp. 6-1-6-43). New York: Wiley.
- Weinstein, G. W., Hobson, R. R., & Dowling, J. E. (1967). Light and dark adaptation in the isolated rat retina. *Nature*, 215, 134–138. [[PubMed](#)]